ELSEVIER
Vailable online at www.sciencedirect.com
SciVerse ScienceDirect
Energy Procedia 27 (2012) 449 – 454
Energy Procedia

SiliconPV: April 03-05, 2012, Leuven, Belgium

Laser doping strategies using SiN:P and SiN:B dielectric layers for profile engineering in high efficiency solar cell

S. Gall[a], B. Paviet-Salomon[a], J. Lerat[b], T. Emeraud[b]

[a]*CEA-INES, Savoie Technolac, BP 332, 50 avenue du Lac léman, 73377 Le Bourget du Lac Cedex France*
[b]*EXCICO Group NV, Kempischesteenweg 305 bus 2, B-3500 Hasselt, Belgium*

Abstract

In this paper an Excimer laser doping process is investigated from SiN:P and SiN:B PECVD layers used as dopant sources. It is demonstrated efficient doping effect with P and B with large doping range on both p^+ and n^+ pre-diffused regions. Doped regions are shown to be modified in term of surface concentration and depth by both laser-driven re-distribution and additional over-doping from doped dielectric source. When using laser doping from SiN:B layer, partial or complete compensation of the initial n^+ emitter is highlighted. Moreover similar study with SiN:P demonstrated the potential for over-compensate the initial p^+ emitter. These laser processes could be used for realization of adjacent p^+ and n^+ regions with controlled profiles. Moreover fluence ranges where material could be fully compensated are pointed.

Keywords: solar cells; ion implantation; phosphorus; passivation; thermal annealing; screen-printing

1. Introduction

Localized doped areas with controlled doping profiles are required for most of advanced high efficiency solar cells on *p*-type or *n*-type silicon substrates, from well-known selective emitter [1] to more complex IBC structures [2]. Commonly used techniques feature high temperature diffusion processes or dopant source deposition followed by furnace or laser annealing [3-4] for P and B doped regions realization. These are followed by localized chemical surface etching steps and/or high temperature drive-in steps to optimize doping profiles. Passivation improvement on both n^+ and p^+ doped regions could be achieved by tuning the dopant surface concentration and re-distributing the initial dopant profiles [1,5,6]. On the particular case of highly doped p-type silicon (e.g. boron emitter), an elegant approach consists in locally over-compensate the surface of the Boron emitter by a shallow Phosphorous surface $POCl_3$ diffusion [7]. Significant emitter saturation current density improvement is demonstrated on compensated surface after thermal SiO_2 passivation and confirmed by V_{oc} value of 676 mV achieved on Emitter Passivated by a Shallow Junction (EPJ) solar cell [7].

Nevertheless these examples of high efficiency structures suffer from process complexity with large

doi:10.1016/j.egypro.2012.07.092

number of technological steps. From an industrial point of view, limitation of steps number and global thermal budget in the full flow of the solar cells are favored.

This paper describes our recent work on dopant profile engineering based on combination of one high temperature diffusion step and additional Excimer laser doping process from SiN_x layers doped with Phosphorus or Boron. First results show that initial p^+ or n^+ doped regions can be tuned either by over-doping with same type of dopant or compensation with opposite dopant type.

2. Experimental

p-type and *n*-type 14-22 Ω.cm Cz shiny-etched substrates with a thickness of 300 µm were used. The *p*-type samples first underwent a 40 Ω/□ $POCl_3$ furnace diffusion, followed by controlled chemical etching to increase n^+ emitter R_{sh} up to 170 Ω/□. Similarly the *n*-type substrates were diffused with 65 Ω/□ BCl_3 process followed by surface etching to increase p^+ emitter up to 100 Ω/□.

Table 1. Emitter samples preparation on p-type and n-type substrates

Substrate	Diffusion		Surface Etching	
	Process	Rsheet [Ω/□]	Etching time [min]	Rsheet [Ω/□]
Cz p-type (14-22 Ω.cm)	POCl3 840°C	40	60	160
Cz n-type (14-22 Ω.cm)	BCl3 940°C	65	60	100

Then samples were covered with 70 nm thick SiN:P or SiN:B layers grown by adding either PH_3 or TMB gas flux respectively during the PECVD deposition standard process of non-doped SiNx layer [5]. Samples were irradiated with a pulsed XeCl excimer laser, with λ=308 nm and σ_p=150 ns. Detailed description of the laser source could be founded in ref [8]. The laser energy density (E_d) was varied between 0 and 6.00 J/cm² and resulted simultaneously in partial or total ablation of the dielectric layer and doping of the underlying substrate. Accurate process control is achieved by real time silicon melting time measurement using time resolved reflectivity (TRR). Irradiated areas were characterized by 4-probes method for R_{sheet} measurement and resulting P and B profiles were analysed by Secondary Ion Mass Spectroscopy (SIMS).

3. Results and Discussion

3.1. Direct doping of non-diffused silicon from SiN:P and SiN:B layers

Laser over-doping of *p*-type and *n*-type polished silicon (Si) substrate were obtained from 70 nm thick SiN:P and SiN:B layers. As can be seen in Fig 1, both layers allow to reach R_{sheet} below 30 Ω/□. Visual observations reveal partial removal and/or chemical modification of the dielectric layer above 0.8 J/cm² for the SiN:P and 1.8 J/cm² for SiN:B. These thresholds correspond to the initial detection of melting time (Fig. 2) highlighting material dependence of laser energy interaction. A longer melting time with the SiN:P layer is observed (~ x3) due to the change in refractive index when P atoms are introduced in SiN layer [5]. Based on similar mechanisms than laser doping from sputtered or spin-on doped layers in the nanosecond regime [9,10], irradiated region of surface is melted thanks to absorption of laser energy, then recrystallized with introduction of dopant atoms under electrical active state. In the present case, doping occurs from P and B atoms available in the SiN:P and SiN:B layers.

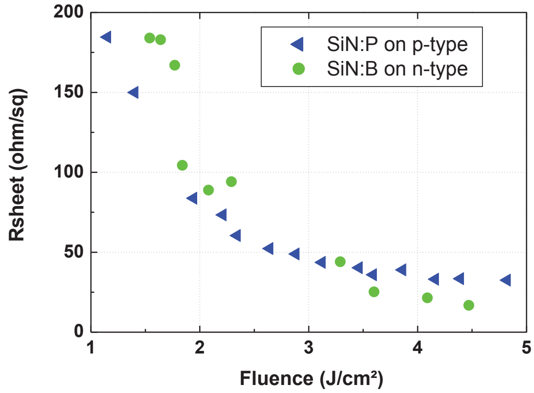

Fig. 1. R_{sheet} evolution after doping from SiN:P and SiN:B versus laser fluence on *p*-type and *n*-type substrates

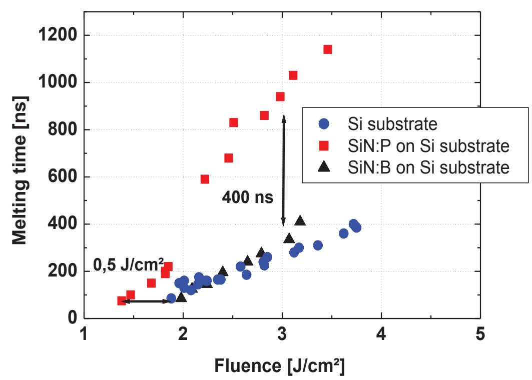

Fig. 2. Melting time versus laser fluence on bare Si substrate and on SiN:P/Si and SiN:B/Si

3.2. Phosphorous over-doping of initial n+ emitter

At first, laser doping from SiN:P is studied when directly deposited on 160 Ω/sq n^+ emitter. Visual observation of the sample after irradiation at increasing fluences reveals slight chemical change of the initial SiN:P layer from 1.0 J/cm² to 2.0 J/cm², then partial removal up to 3.2 J/cm² and finally complete ablation above 3.2 J/cm². Sheet resistance values measured after HF treatment (Fig. 3) decreases first slowly from initial R_{sheet} to 140 Ω/sq. Then R_{sheet} decreases sharply up to 3.8 J/cm² to reach a plateau around 50 Ω/□ at higher fluences. The R_{sheet} vs laser fluence curve behaviour is similar to the case of laser over-doping from Phosphosilicate Glass (PSG) remaining after $POCl_3$ diffusion. In the present case, neither the PSG nor the high doped “dead zone” are present and can act as dopant source. On the other hand the strong slope of the R_{sheet} curve between 2.5 and 3.5 J/cm² confirms effective over-doping from SiN:P doping source in that range. At higher fluence all the Phosphorous atoms available in the SiN:P layer have been diffused, and the doping layer itself has been removed. Longer melting time measured at higher fluence induces deeper silicon liquid phase and in turn in-depth profile redistribution. This hypothesis correlates with R_{sheet} value conservation above 3.8 J/cm².

SIMS Phosphorous profiles after irradiation at various fluences are presented on Fig. 4. At 1.6 J/cm², doping from SiN:P is obvious since the profile appears deeper and more surface concentrated than the initial n^+ emitter. After irradiation at 3.2 J/cm², the profile is deeper but presents same surface concentration. From 3.2 to 3.8 J/cm², surface concentration increase from 3.8E19 at/cm^3 to 6.4E19 at/cm^3 but depth remains almost the same. Finally a fluence of 5.0 J/cm² induces deeper but less concentrated profile. At energy higher than 3.8 J/cm², all the dopant atoms have been introduced in the silicon but deeper melted region increase profile depth by reducing surface concentration.

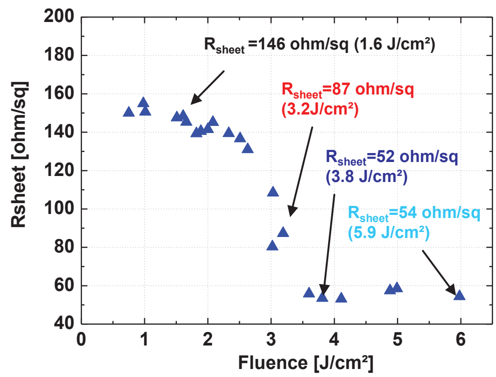

Fig. 3. Sheet resistance evolution after irradiation of SiN:P layer deposited on 160 Ω/sq initial n^+ emitter

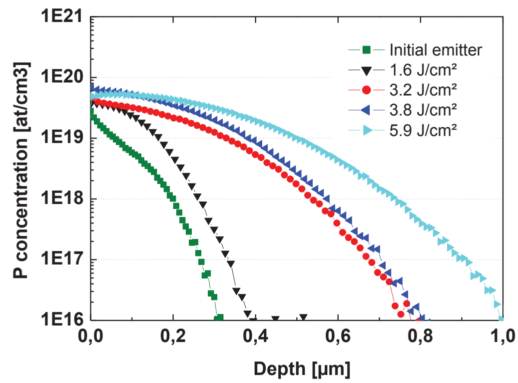

Fig. 4. SIMS Phosphorous profiles of initial emitter and after irradiation at 1.6, 3.2 and 3.8 J/cm²

3.3. *Boron compensation of initial n^+ emitter*

Similar study is performed when a SiN:B layer is deposited on the initial n^+ emitter. As shown on Figure 5, the R_{sheet} remains almost constant up to 2.3 J/cm² and then increases between 2.5 and 3.4 J/cm² to reach 280 Ω/□. In a last time R_{sheet} sharply decreases down to a 40 Ω/□ plateau. We explain this up and down behavior as follow: when fluence increases, more and more Boron atoms are diffused in the silicon. At low doping level, even if Boron concentration remains minoritary as compared to Phosphorous, they contribute to balance the n^+ emitter and the R_{sheet} value increases slowly. As soon as B concentration equals P concentration, positive and negative electrical free charges annihilate themselves and the material becomes electrically insulator, highlighted by a R_{sheet} raise. At higher fluence, Boron atoms over-compensate the initial n^+ emitter, the doped region become majoritary *p*-type and R_{sheet} decreases.

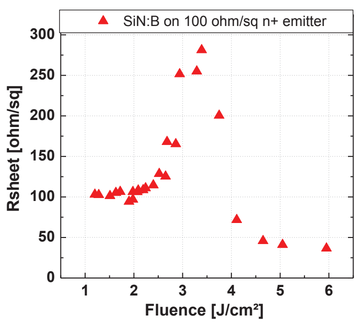

Fig. 5. R_{sheet} evolution after doping from SiN:B deposited on 100 Ω/□ n^+ emitter

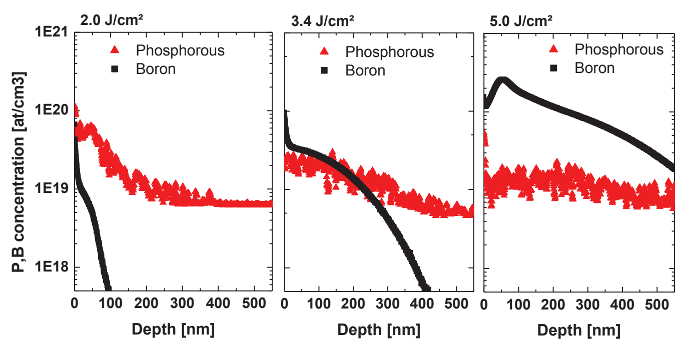

Fig. 6. P and B SIMS profiles after irradiation at 2.0, 3.4 and 5.0 J/cm² of SiN:B layer deposited on n^+ emitter

This hypothesis is partially confirmed by P and B SIMS profiles presented on Fig. 6 (P profiles present a poor depth resolution because of non optimized acquisition condition). Shallow Boron doping is confirmed at 2.0 J/cm² but concentration remains low as compared with P profile. At 3.4 J.cm², B surface concentration (3E19 at/cm^3) slightly exceeds P concentration (1E19 at/cm^3) but it could be believed that both active concentrations are similar and electrical free charges are annihilated. At 5.0 J/cm², B profile presents a surface concentration below 1E20 at/cm^3 with 1 µm depth and the Phosphorous profile has been in-depth redistributed. Also is seen a local minimum on the B profile already described in the literature [7]. Initial n^+ emitter has been over-compensated and becomes *p*-type.

3.4. Phosphorous compensation of initial p^+ emitter

The case of boron over-doping of p^+ emitter has been studied and shows similar mechanisms than those seen when SiN:P is deposited on n^+ emitter (see 3.2). R_{sheet} decreased from initial value of p^+ emitter (100 Ω/□) to a 30 Ω/□ plateau with the same 3 typical R_{sheet} slope changes. Finally we focused our study on Phosphorous compensation of p^+ emitter. The R_{sheet} shows slight increase up to 2.5 J/cm², then sharply increases between 2.5 and 3.6 J/cm² to reach a R_{sheet} close to 450 Ω/□. At higher fluence R_{sheet} strongly decreases to reach a plateau around 50 Ω/□. This up and down behaviour could be explained by similar mechanisms described in the opposite case, i.e. Boron compensation of n^+ emitter. At low fluence the initial p^+ emitter is partially redistributed with slight doping from SiN:P. More and more P atoms are introduced in the silicon matrice with P concentration close to initial B level of p^+ emitter. When [B]~[P], the R_{sheet} increases because the doped region is compensated. At higher fluence, P concentration of active dopants becomes higher to B concentration and the doped region becomes mainly n-type. Such hypothesis is confirmed by the SIMS profiles measured at typical 1.3, 2.0, 3.6 and 4.1 J/cm² presented on Fig 6.

At 1.34 J/cm², the Boron profile presents a 1E20 at/cm^3 surface concentration and 0.35 µm depth. Also is observed a sharp and shallow Phosphorous profile with low surface concentration induced by laser doping effect from the SiN:P layer. The Boron profile after irradiation at 2.0 J/cm² has been strongly redistributed with reduced surface concentration and profile depth around 0.7 µm. The Phosphorous profile shows a highly concentrated surface on the first 0.1 µm and then a 0.4 µm deep and low concentrated tail. Nevertheless the P atoms introduced in the silicon could explain the slight R_{sheet} increase (R_{sheet}=100 Ω/□). At 3.6 J/cm², the B profile has surface concentration close to 4.5 E19at/cm3 with a local minimum already described by Benick et al. [7] when boron surface is locally over compensated by Phosphorous. The P profile shows a 1E20 at/cm^3 concentrated surface with a 0.8 µm depth. This fluence corresponds to the compensated material where the R_{sheet} presents a nearly 450 Ω/□ value. It could be concluded that the initial p^+ emitter is almost compensated by Phosphorous atoms introduced by the laser process. At 4.1 J/cm², both profiles appeared deeper but the P active concentration should be higher since the R_{sheet} shows strong decrease.

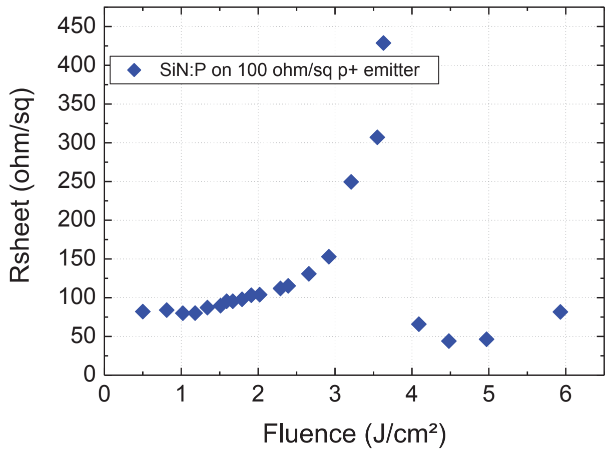

Fig. 7. R_{sheet} evolution after doping from SiN:P deposited on 100 Ω/☐ p^+ emitter

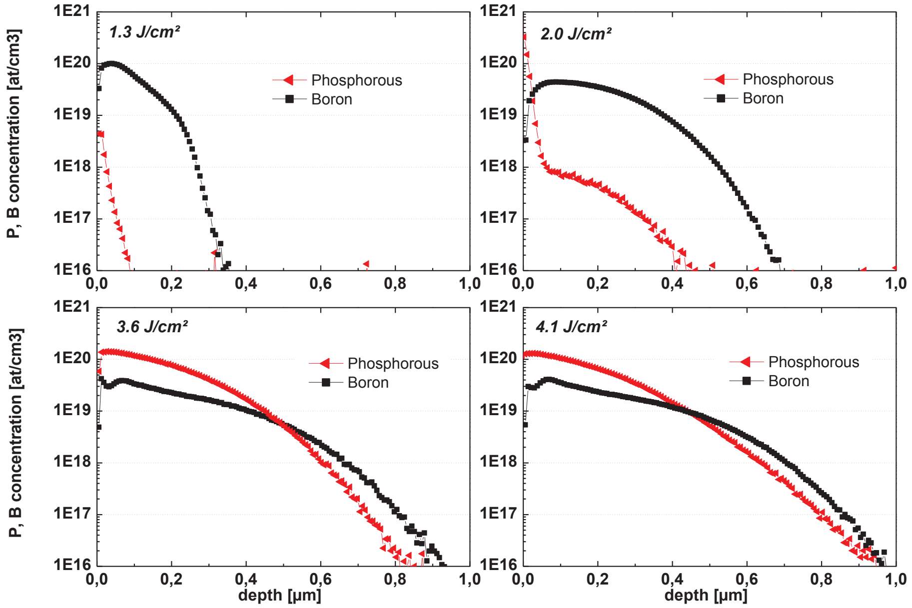

Fig. 7. R_{sheet} evolution after doping from SiN:P deposited on 100 Ω/☐ p^+ emitter

4. Conclusion

In this paper P and B laser doping of both p^+ and n^+ emitters is investigated from SiN:P and SiN:B layers used as dopant source. It has demonstrated a large range of doping level on non-diffused substrate, up to 30 Ω/□ for n^+ and 15 Ω/□ for p^+ regions. In addition we show over doping of pre-diffused n^+ and p^+ emitter from SiN:P and SiN:B layers respectively. We demonstrated partial and complete compensation of the initial doped regions by laser doping with opposite dopant type. These laser processes could be suitable to realize by a simple way complex photovoltaic structures with adjacent p^+ and n^+ regions separated by isolating area.

References

[1] B. Paviet-Salomon et al., Proc. 26th European Photovoltaic Solar Energy Conference (WIP Munich 2011) pp. 1365-1368
[2] C. Gong, IEEE Electron Device Letters. Vol. 31, NO.6, June 2010
[3] E. Fogarassy et al., J. Appl. Phys. 52, 1981, pp.1076-1082.
[4] T. Sameshima et al.,, J. Appl. Phys. 62, 1987, pp.711-713.
[5] S. Gall et al., PVSEC, Proc. 26th European Photovoltaic Solar Energy Conference (WIP Munich 2011) pp. 576
[6] P. Cousins et al., IEEE Photovoltaic Specialists Conference 2010.
[7] J. Benick et al. Proc. 23th European Photovoltaic Solar Energy Conference (WIP Munich 2008) pp. 1550-1553
[8] S. Gall et al., 25th European Photovoltaic Solar Energy Conference (WIP Munich 2010) pp. 1852-1854
[9] S. Eisele at al. Proc. 24th European Photovoltaic Solar Energy Conference (WIP Munich 2009)
[10] H. Kerp et al., International Photovoltaic Solar Energy Conference, 2005